Martinez-Calderon *et al.*
Earth, Planets and Space (2021) 73:191
https://doi.org/10.1186/s40623-021-01516-y

Earth, Planets and Space

FULL PAPER Open Access

A review of unusual VLF bursty-patches observed in Northern Finland for Earth, Planets and Space

Claudia Martinez-Calderon[1*], Jyrki K. Manninen[2], Jemina T. Manninen[2] and Tauno Turunen[2]

Abstract

Using numerical filtering techniques allowing us to reduce noise from sferics, we are able to clearly study a new type of differently structured very low frequency (VLF) radio waves above f = 4 kHz at the ground station of Kannuslehto in northern Finland (KAN, MLAT = 64.4°N, L = 5.5). These emissions are intriguing, since they are detected at frequencies above half the electron gyrofrequency in the equatorial plane (f_{ce}) for the L-shell of Kannuslehto (f_{ce} ~ 5–6 kHz). They are commonly observed at Kannuslehto, but have also been infrequently reported at other stations, sometimes under different names. Their possible common origin and manner of propagation is still under investigation. This paper unifies the nomenclature by regrouping all these waves detected at frequencies higher than the local equatorial 0.5 f_{ce} at the L-shell of observation under the name of VLF bursty-patches. While these waves have different spectral features, they appeared mostly composed of hiss bursts with durations of a few seconds to several minutes. They also show periodic features with varying periodicity and shape. They are sometimes characterized by single bursts covering very large frequency ranges of several kHz. We also give a review of the different characteristics of VLF bursty-patches observed at Kannuslehto, which at the moment, is the station with the highest observation rate. We present recent observations between 2019 and 2021.

Keywords: VLF waves, Magnetospheric waves, ELF/VLF, VLF bursty-patches

Introduction

Earth's magnetic field interacts with the solar wind to create a cavity called the magnetosphere, protecting us from harmful energetic particles of solar origin. However, this cavity is not entirely hermetic, allowing a certain quantity of energetic electrons and protons from the solar wind to penetrate the magnetosphere. These particles are then trapped around the Earth in what is commonly known as the radiation belts or Van Allen belts. Through resonant cyclotron interactions, electrons up to several tens of keV are behind the generation of extremely low (ELF) and very low frequency (VLF) emissions. These emissions are plasma waves in the whistler-mode that propagate below the local gyrofrequency of electrons (Kennel and Petschek 1966; Helliwell 1965; Gurnett and Bhattacharjee 2017). Their names come from the frequency band in which they are detected: between 0.3 and 3 kHz for ELF and 3 to 30 kHz for VLF (Barr et al. 2000).

Historically, ELF/VLF waves have been categorized by their spectral features (Helliwell 1965). For example, emissions showing discrete elements with rising or falling frequency tones in the timescale of tenths of seconds are known as chorus (Sazhin and Hayakawa 1992; Santolik 2008 and references therein). These are usually the most common and intense type of ELF/VLF waves. On the other hand, noise-like broadband emissions with no discernible discrete features are called hiss (see reviews by Sazhin et al. 1993; Hayakawa and Sazhin 1992). If the waves present a periodic time modulation of their intensity in the orders of several seconds up to minutes they

*Correspondence: claudia@isee.nagoya-u.ac.jp
[1] Institute for Space-Earth Environmental Research, Nagoya, Japan
Full list of author information is available at the end of the article

are classified as quasi-periodic (QP) (e.g., Sazhin and Hayakawa 1994; Smith et al. 1998). In this manner, several types of VLF waves have been previously classified and documented, first using ground-based data and more recently using satellite measurements.

While in space, VLF waves are usually clearly observed, however on the ground the measurements are often polluted by electromagnetic noise, either of natural or human origin. In particular, sferics originating from lightning discharges present themselves as a multitude of vertical lines almost completely covering frequencies above 4 or 5 kHz on spectrograms. During the periods of high lightning storm activity these sferics can cover all the frequencies down to 1 kHz obscuring the observations of VLF emissions. To improve the study of VLF waves by ground-based receivers, the Sodankylä Geophysical Observatory (SGO) in Finland developed a sferics filtering system (briefly explained in Manninen et al. 2016). While this process has ameliorated the observations of usual VLF emissions, such as chorus and hiss on the ground, it also allowed for the clear study of frequencies above 5 kHz, where a new type of VLF emissions was observed.

Using data from the VLF-CHAIN campaign in February 2012, Shiokawa et al. (2014) reported the existence of 'Bursty-Patch' emissions at the ground station of Athabasca, Canada (ATH, MLAT = 64.5, L ~ 4.3) during geomagnetically disturbed periods. These were short duration bursty emissions observed above 4 kHz, sometimes at frequencies higher than the usual half gyrofrequency of electrons (f_{ce}) in the equatorial plane of the magnetosphere at the L-shell of ATH (0.5 $f_{ce\ eq.}$ = 5.5 kHz). These type of observations are of notice as waves detected at frequencies higher than the local 0.5 f_{ce} indicate these waves are not traveling ducted in a geomagnetic field aligned enhancement of electron density (Carpenter, 1968; Inan and Bell, 1977). At f > 0.5 f_{ce}, the waves would be traveling with oblique wave angles with respect to the local magnetic field lines, also known as unducted propagation (e.g., Němec et al. 2013; Titova et al. 2017; Martinez-Calderon et al. 2016). It is believed that in the latter case, detection on the ground becomes more difficult as the waves might have more difficulties crossing the ionosphere, because their wave normal angles with respect to the vertical can become very large. Since bursty-patches consisted of short duration rising-tone elements and were consistent with the expected upper frequency band of chorus, they believed these two emissions to be linked. Using polarization analysis, Martinez-Calderon et al. (2015) showed that the main chorus emissions accompanying bursty-patches were likely coming from two separate locations in the ionosphere. In addition, bursty-patches were usually detected at ATH as coming from very similar directions. This analysis could not confirm with certainty if bursty-patches and chorus were linked or generated by a separate source. Since ATH data is usually obscured by sferics, further study of these type of emissions could not be accurately completed.

Thankfully, the data from the VLF receiver at Kannuslehto [KAN, MLAT = 64.4, L ~ 5.5] in Northern Finland, has been analyzed with a sferics filter allowing for clearer observations at frequencies above the local 0.5 $f_{ce\ eq}$ at the L-shells of KAN (0.5 $f_{ce\ eq}$ = 2.7 kHz). KAN not only observed emissions similar to the bursty-patches as described by Shiokawa et al. (2014), but also detected multiple other types at unusually higher frequencies, above the local equatorial gyrofrequency ($f_{ce\ eq.}$ = 5.4 kHz). Manninen et al. (2016) made a first report of these type of unusually high frequency natural VLF emissions without focusing on their different characteristics but grouping them together as RREs (i.e., recently revealed emissions). They showed that these emissions are a dayside phenomenon, peaking close to local noon. They were detected on 78% of all campaign days between 2006 and 2016, and seem to be mostly hiss-like in nature. While the mechanisms behind their generation and propagation remain mostly unknown, they could be generated due to self-oscillations in the magnetospheric maser and should originate at L-shells lower than the position of KAN (Manninen et al. 2017).

Even though these unusual high frequency emissions tend to look like hiss bursts, on closer inspection they show a wide variety of spectral shapes. In some cases, they are shaped like bullets with sudden stops or show wing-like features, while in other cases, we note gradual frequency increase or showing multiple periodic features (Manninen et al. 2016, 2017). More recently, Manninen et al. (2021) described these type of emissions as high-frequency VLF patches or VLF 'birds' and focused on their relationship to temporal and spatial details of wave–particle interactions. They noticed that these waves were only observed at times of no or weak space weather conditions. They concluded that VLF-patches could indirectly indicate a local enhancement of electron fluxes and could be generated even if they were not being detected on the ground. While we understand a bit more on these waves, the reasons behind this variety of shapes or periodicity mechanisms are still unknown.

In this paper, we will focus on remarkable observations of high frequency VLF emissions at the ground station of KAN from 2019 to 2021, and particularly those detected above 6 kHz, i.e., f > f_{ce}. We will discuss some features that have not been previously reported, as well as a closer look at a few particular types of periodic emissions and consider possible mechanisms behind the observed characteristics. This paper also aims to unify the nomenclature

for these new group of VLF emissions which have often been called by different names in several papers and presentations: RREs, 'birds', 'bursty-patches', VLF bursts, VLF patches and KHF-VLF. These unusual type of high frequency emissions observed at $f > f_{ce}$ will be known as ***VLF bursty-patches***.

Data

In this study we present data from a VLF receiver located in the auroral zone of Northern Finland at KAN. The station is located at a latitude of 67.74 N, a longitude of 26.27 E, and at the L-shell of 5.5. The receiver itself is made of two separate square loop antennas measuring the magnetic field variations in the east–west and north–south directions with a sampling frequency of 78.125 kHz and a sensitivity of about 0.1fT (Manninen 2005). The configuration and location of the receiver has been the same since 2006.

Data from KAN benefits from a unique sferics filtering system. When we apply the sferics filter during the data analysis, we allow between 15 and 20% data loss. Meaning that while we are able to reduce the noise from sferics, we do not remove them all as otherwise the VLF emissions at these frequencies would also be removed. Therefore, noise from sferics is still moderately visible in most the figures shown below.

KAN is run on a campaign basis, and the duration of the campaigns have been from a week up to a month from 2006 to 2013. From 2014, the campaign observation days have been slowly increased in number to cover measurements from optical data and satellites (especially Arase, launched in December 2016). Since 2017 the campaigns usually cover the winter months and the receiver is turned off during the arctic summer to avoid thunderstorms and the midnight sun. For this study we processed data from the 2019–2020 and 2020–2021 winter campaigns, but also give general occurrence of VLF bursty-patches since 2016. We show selected cases between 2019 and 2021 to illustrate different types of spectral features of VLF bursty-patches in the time frame of several hours.

General characteristics

Definition of VLF bursty-patches

While these type of emissions have been reported before under different names, this paper aims to (1) unify their naming convention, (2) present their main characteristics and (3) review their most recent observations.

We define VLF bursty-patches as whistler-mode VLF waves detected at frequencies higher than the local equatorial 0.5 f_{ce} at the L-shell of the ground station in which they are observed. To distinguish them from upper band emissions, we also stipulate that if they are observed at $0.5\, f_{ce} < f < f_{ce}$, they should also show no correspondence with 'usual' waves observed at lower frequencies below 0.5 f_{ce}.

Figure 1 shows the power spectrum density at the ground station of KAN between 0 and 10 kHz on 1 October 2020 from 06:00 to 10:00 UT. The magnetic local time (MLT) at KAN is UT + 1.5 h, hence these observation timings correspond to 07:30–11:30 MLT. The white dashed lines indicate the average half gyrofrequency for electrons at the equator at the L-shell of KAN (0.5 f_{ce}), while the dotted line indicates the average gyrofrequency (f_{ce}). This figure shows multiple emissions at different frequencies, including 'usual' VLF emissions at lower frequencies and typical examples of VLF bursty-patches for $f > 0.5\, f_{ce}$.

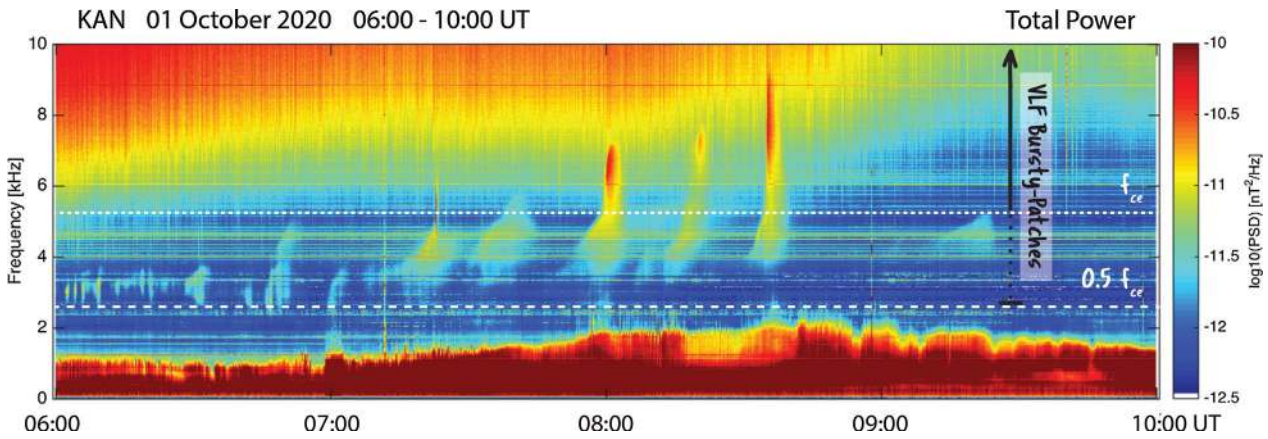

Fig. 1 Definition of VLF bursty-patches at KAN. Power spectrum density at KAN on 1 October 2020 from 06:00 to 10:00 UT (07:30–11:30 MLT). Dashed and dotted horizontal white lines show, respectively, the local equatorial 0.5 f_{ce} and f_{ce} for the L-shell of KAN. VLF bursty-patches are observed at 2.7–4 kHz from ~ 06:00 to 07:10 UT, and at 3–9 kHz from ~ 06:50 to 09:30 UT

We note that from 06:00 to 09:00 UT in Fig. 1, there are multiple vertical lines overlapping at frequencies above 6 kHz. These are very strong emissions that correspond to noise from sferics ("Data" Section), and are not the focus of this study. Below ~ 2 kHz, slightly under the dashed 0.5 f_{ce} line, we observe a hiss emission accompanied by burst or quasi-periodic elements. This illustrates 'usual' VLF emissions at KAN, detected at $f < 0.5\, f_{ce}$, which will generally be neglected unless their features are relevant to the discussion on VLF burst-patches.

The main target of this study is between the two white lines ($0.5\, f_{ce} < f < f_{ce}$) in Fig. 1, where we can distinguish two groups of VLF bursty-patches. The first group globally in the first hour of observation, stays between ~ 2.7 and 4 kHz, below f_{ce}. This group presents itself as several hiss bursts of varying duration. At these frequencies they could correspond to upper-band emissions but do not seem to share the same burst timings as those waves observed below 1 kHz. More interestingly, the second group of VLF bursty-patches are detected from ~ 06:50 until 09:30 UT between approximately 3 and 9 kHz. The emissions are also hiss-like bursts, however, they last tens of minutes and show increasing intensity and frequency with time. Their slope also changes, as it appears to become steeper with time becoming almost vertical, except for the last burst at ~ 09:15 UT.

General occurrence of VLF bursty-patches

Manninen et al. (2016) showed the occurrence of VLF bursty-patches detected between 4 and 15 kHz at KAN for the observation campaigns between 2006 and 2016. Over this period, VLF bursty-patches were observed at different phases of the 11-year solar cycle and on ~ 78% of all campaign days. Here, we complement these statistics by including the occurrence of VLF bursty-patches for 2016–2021. Table 1 shows the general occurrence of VLF bursty-patches separated by year, from 2016 until April 2021. As KAN operates on a campaign basis and it's not active all year long, we indicate for each year, the total campaign observation days and the percentage of these days, where VLF bursty-patches were detected.

Looking at Table 1, considering the results from 2016 onwards, we note a decreasing trend, with VLF bursty-patches only detected on ~ 43% of the campaigns days in 2017, compared to ~ 70% the year before. We reach a local occurrence minimum at ~ 10% of observation days for 2018. From 2019 onwards, the trend is reversed with increasing occurrence rates year after year. Respectively, VLF bursty-patches occurrence rates for 2019, 2020 and 2021 are ~ 19% 27 and 46% of the campaign observation days (we note the 2021 campaign only considers data up to end of April 2021, corresponding to about half of the usual data for a year).

These numbers show that VLF bursty-patches are not a rare occurrence and are observed quite frequently at KAN, also supporting recent results by Manninen et al. (2021). On the other hand, other studies have reported VLF bursty-patches at other ground stations (e.g., Shiokawa et al. 2014; Martinez-Calderon et al. 2015) but they are only mentioned as few selected cases. The lack of statistics or studies discussing their general occurrence show that they are not as commonly observed as at KAN. This can be explained by both the high sensitivity of the VLF receiver at KAN (Manninen 2005; Manninen et al. 2016) and their automatic implementation of the sferics filter. Since other ground-stations do not have implemented their own sferics filter as a rule for all their observations, it is likely that scientists are unable to observe VLF bursty-patches regularly in their data sets. They can only report the cases observed during particularly noiseless day or events that are strong enough to be observed through the sferics. We do note that some ground-stations focused on the study of whistlers, use a type of sferics filtering in their Automatic Whistler Detector Algorithm and Automatic Whistler Analyzer. However, since both algorithms are automatic and target whistlers, the preprocessed files are not studied, and therefore, any possible observations of VLF bursty-patches are not reported (Lichtenberger et al. 2008, 2010).

In addition, because of the sferics noise most of these observations can also only be limited to the frequency range of $0.5\, f_{ce} < f < f_{ce}$ and an observer could dismiss such observations as related to upper band chorus for example. The differences of observations of VLF bursty-patches at KAN and other ground stations can also reflect different propagation or generation properties at different locations. However, this can only be more accurately determined if the other observation points also

Table 1 General occurrence of VLF bursty-patches from 2016 to 2021

	2016	2017	2018	2019	2020	2021(*)
Total campaign observation days	113	216	241	206	223	120
VLF bursty-patches observation days	80	93	23	39	59	58
Percentage of campaign days with detection of VLF bursty-patches	70.8%	43.1%	9.5%	18.9%	26.5%	48.3%

Summary of the observation of VLF bursty-patches compared to observation day at KAN for 2016–2021. (*) Only takes into account the data up to end of April 2021

apply a sferics filter to try to reduce the bias due to the sferics noise covering higher frequencies.

Most of the VLF bursty-patches observed at KAN had right handed polarization, suggesting that the station detected them directly after they exited the ionosphere and ruling out long propagation in the Earth-Ionosphere wave guide (e.g., Ozaki et al. 2008; Martinez-Calderon et al. 2015, 2021). This is also supported by the high wave intensity of the bursty-patches (at least 2 orders of magnitude greater than the background), indicated it is unlikely the waves traveled long enough in the wave guide to be damped. We also note that the angle of arrival of the waves at KAN (not shown here) show the signals coming from all directions, i.e., the waves did not propagate a long distance in the wave guide, otherwise we would expect to see them all incoming southwards of the station.

As shown in Table 1, the occurrence of VLF bursty-patches at KAN shows a global decrease reaching a local minimum in 2018, following by a steady increase in the following years. This seems to be in agreement with the solar cycle 24 whose minimum was also in 2018, suggesting that VLF bursty-patch generation or propagation are affected by the solar cycle. Previous studies also found that VLF bursty-patches are mostly observed during quiet space weather conditions at times of small negative Dst values (Manninen et al. 2021). To understand how solar wind condition affect VLF bursty-patches we need to focus on statistics and their relation to solar wind parameters which are outside of the scope and this paper and will be the subject of a separate study.

Examples of VLF bursty-patches at KAN

In this section we will present different types of VLF bursty-patches that are commonly observed at KAN. While some of these cases might have reported before, we show their different characteristics and features in the time frame of hours and with a few selected examples from the most recent KAN campaigns (2019–2021). The names for the observations given below were chosen to reflect the spectral features we wanted to showcase.

Rounded VLF bursty-patches

Figure 2a shows the power spectrum density at KAN on 7 January 2019 from 07:00 to 11:00 UT (08:30–12:30 MLT) for frequencies between 0 and 12 kHz. In a similar format as Fig. 1, the white dashed and dotted lines show the equatorial $0.5\,f_{ce}$ and f_{ce} at the field line of KAN, respectively. Subsequent figures will show these lines to allow for easier identification of VLF bursty-patches. To avoid repetition, we will omit this from future image descriptions.

Figure 2a shows multiple 'usual' hiss and chorus emissions below f_{ce}, but we focus on the discrete VLF bursty-patches observed at f > 8 kHz (observation timings indicated by magenta lines on top of the spectrum). A first group shows multiple round-shaped bursts from ~ 07:20 to 07:50 UT. The clearest band of these rounded emissions is between 9 and 10 kHz with a first burst followed by 4 more closely spaced bursts a few minutes later. Figure 2b shows a more detailed look of these bursts by focusing on the time frame between 07:37 to 07:42 UT. As we zoom in to a time scale of several minutes we note that the bursts lose their round shape and seem to be unstructured in nature, with no visible discrete elements.

Similar rounded bursts are also observed at ~ 10.5 and 11.5 kHz within the same time frame, with a hiss-like burst at 11.5 kHz between ~ 07:50 and 08:05 UT. A second and third group of rounded VLF bursty-patches are observed between 10 and 11.5 kHz, starting at 09:15 UT (with 5 bursts) and at 10 UT (3 bursts). Compared with the first group before 08:00 UT, these VLF bursty-patches are more distributed in frequency appearing slightly less rounded in shape.

None of these groups show corresponding bursts observed at lower frequencies. Although we observe bursts centered at 4 kHz after 09:00 UT, they do not show much similarity or one to one correspondence. This would suggest that the source region for these rounded VLF bursty-patches is separate from that of the emissions at lower frequencies. It is also interesting that while the shape of the bursts changes somewhat in time, the repetition period of a few minutes seems to be similar in all groups. It is possible that the mechanism behind the periodicity could be the same in all cases, while the mechanism responsible for their shape might evolve in time or correspond to distinct sources.

Long lasting VLF bursty-patch hiss band

Figure 3a shows the power spectrum density on 03 April 2020 from 06:30 to 10:30 UT (08:00–12:00 MLT) between 0 and 10 kHz observed at KAN. Similarly, to the previous figure, a hiss-band is present for the entire panel below 1 kHz. It is also accompanied by chorus-like bursts clearly visible in the first and last hour of observation below the $0.5\,f_{ce}$ dashed line. Between ~ 07:00 and 08:00 UT we also note multiple VLF bursts between 2 and 3.5 kHz almost centered at the $0.5\,f_{ce}$ line. Figure 3b shows a snapshot of these two emissions between 07:55 and 07:59 UT. We note the very unstructured hiss-band at higher frequencies, while the lower frequency bursts show somewhat discrete features. While the latter could be VLF bursty-patches, they could also correspond to

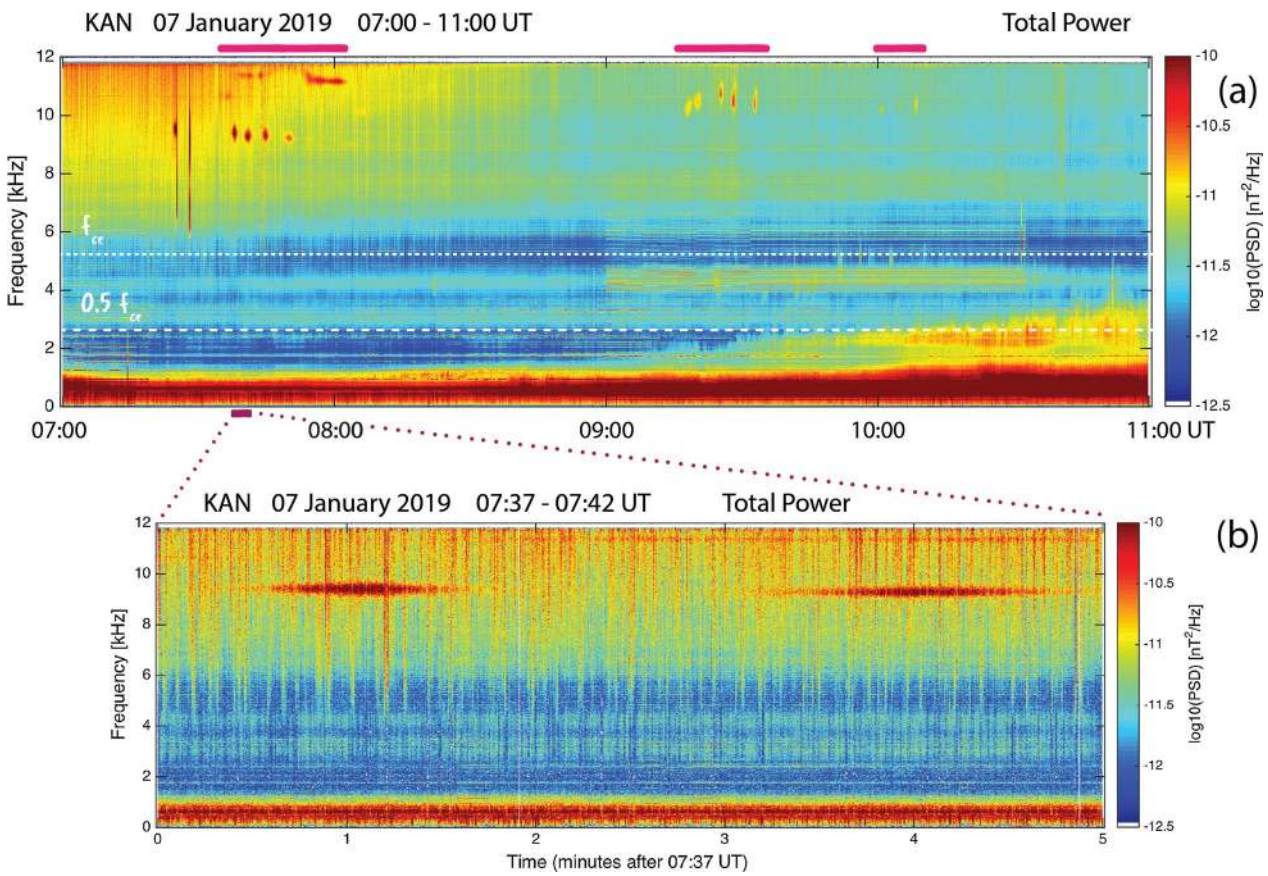

Fig. 2 Example of rounded VLF bursty-patches observed at KAN. Power spectrum density at KAN on 7 January 2020 from **a** 07:00 to 11:00 UT (08:30–12:30 MLT) and from **b** 07:37 to 07:42 UT, between 0 and 12 kHz. Dashed and dotted horizontal white lines show, respectively, the local equatorial 0.5 f_{ce} and f_{ce} for the L-shell of KAN. Three VLF bursty-patches are observed above 8 kHz from ~ 07:20 to 08:10 UT, ~ 09:10 to 09:40 UT and ~ 10:00 to 10:15 UT

upper band chorus bursts propagating to KAN, therefore, they will not be considered for this example.

Here we focus on the long lasting hiss-band VLF bursty patch observed between 5 and 7 kHz mostly above the f_{ce} line. The most important feature of this emissions is that it appears as a continuous band lasting 3 h, from almost the start of the panel up until 09:30 UT. If we consider the two other bursts as part of the same emission, then it adds an additional 40 min. We note that this emission shows no correlation neither with the other discrete VLF bursty-patches at lower frequencies nor with the usual hiss and chorus below the 0.5 f_{ce} line.

Such type of hiss-like VLF bursty-patches lasting up to several hours are not infrequent at KAN. As we will discuss further, there are multiple cases in which VLF bursty-patch events with similar, or sometimes different spectral features, last for several hours. The long duration of these events would suggest these waves could have specific source characteristics (co-rotating with the Earth) or a large generation region with particular propagation characteristics allowing for long-lasting unducted propagation to KAN.

'Wand' VLF bursty-patches

Figure 4a shows the power spectrum density observed at KAN on 23 December 2020 from 04:00 to 08:00 UT (05:30–09:30 MLT) between 0 and 10 kHz. At frequencies below 0.5 f_{ce} we note a constant hiss band at f < 1 kHz and multiple chorus bursts between 0.5 and 2.6 kHz. In the first 30 min we also observe a secondary hiss-like band with multiple short and frequency-elongated bursts starting around 2.5 kHz and up to 6 kHz. While this could correspond to VLF bursty-patches they could also correspond, in part, to the upper band of the chorus emission observed below 2.6 kHz. As such, we will not discuss these events in this example. We also note that the square-like signal present just before 07:00 UT between ~ 1 and 6 kHz is artificial noise due to the ZEVS Russian transmitter located in the Kola Peninsula (< 500 km east of KAN).

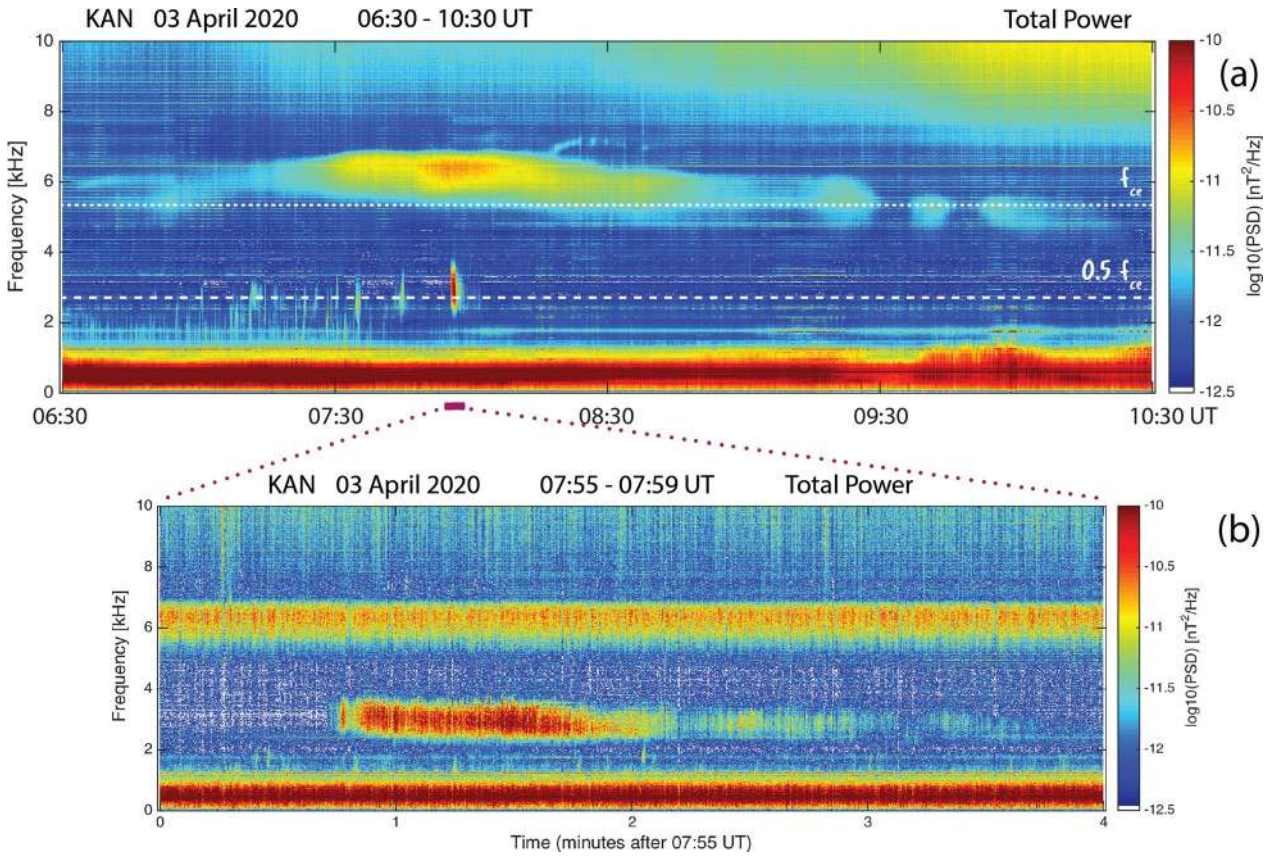

Fig. 3 Example of long lasting hiss-like VLF bursty-patches at KAN. Power spectrum density at KAN on 03 April 2020 from **a** 06:30 to 10:30 UT (08:00–11:30 MLT) and from **b** 07:55 to 07:59 UT, between 0 and 10 kHz. Dashed and dotted horizontal white lines show, respectively, the local equatorial 0.5 f_{ce} and f_{ce} for the L-shell of KAN. Short VLF bursty-patches are observed from ~ 07:00 to 08:00 UT. A long-lasting hiss-like VLF bursty-patch is observed at 5–7 kHz for almost the entire 4 h

Here we focus on a relatively common type of VLF bursty-patch emission that appears as multiple frequency-elongated events similar to large sticks or wands in the 1-h time scale. They are visible for most of Fig. 4a between approximately 5–9.5 kHz, even though in some cases they extend a bit further in frequency. To identify these VLF bursty-patches more easily we have highlighted some examples with black angle arrows on top of the many bursts above the f_{ce} line in Fig. 4a. These events are observed semi-continuously for the entire duration of the panel corresponding to 4 h. These VLF bursty-patches are characterized by their short time duration, only a few minutes, and their rather large frequency range (typically 2 kHz or more) giving them a wand-like appearance. Figure 4b shows this smaller time frame by focusing on one of this 'wands' between 07:44 and 07:47 UT. Here, we confirm that the wand covers the 5–9 kHz range and shows a hiss-like structure with rising tones. In the last minute of Fig. 4b, we also note what appears to be two separate frequency bands that could make us recall chorus emissions. However, since we are at much higher frequencies than 0.5 f_{ce} it is more likely that this could be the result of overlapping emissions.

'Wands' are a common type of VLF bursty-patches and are observed quasi-continuously in different time-scales, from a few minutes to multiple hours, as illustrated in Fig. 4a. In some cases, they also show a kind of periodicity related to a yet unknown mechanism. Their observations are also very stable in frequency, with most of the 'wands' staying in similar frequency ranges. In the case shown here, most of the bursts are concentrated between 7 and 8 kHz.

The characteristics mentioned above could suggest that these 'wands' are generated by a same source that is active for several hours and possibly co-rotating with the Earth. In the following hours after 08:00 UT (not shown here), the VLF bursty-patches disappear for 1 h and are then followed by the appearance of QP elements at the same frequencies for several minutes. If there is a relationship between the 'wands' and QP

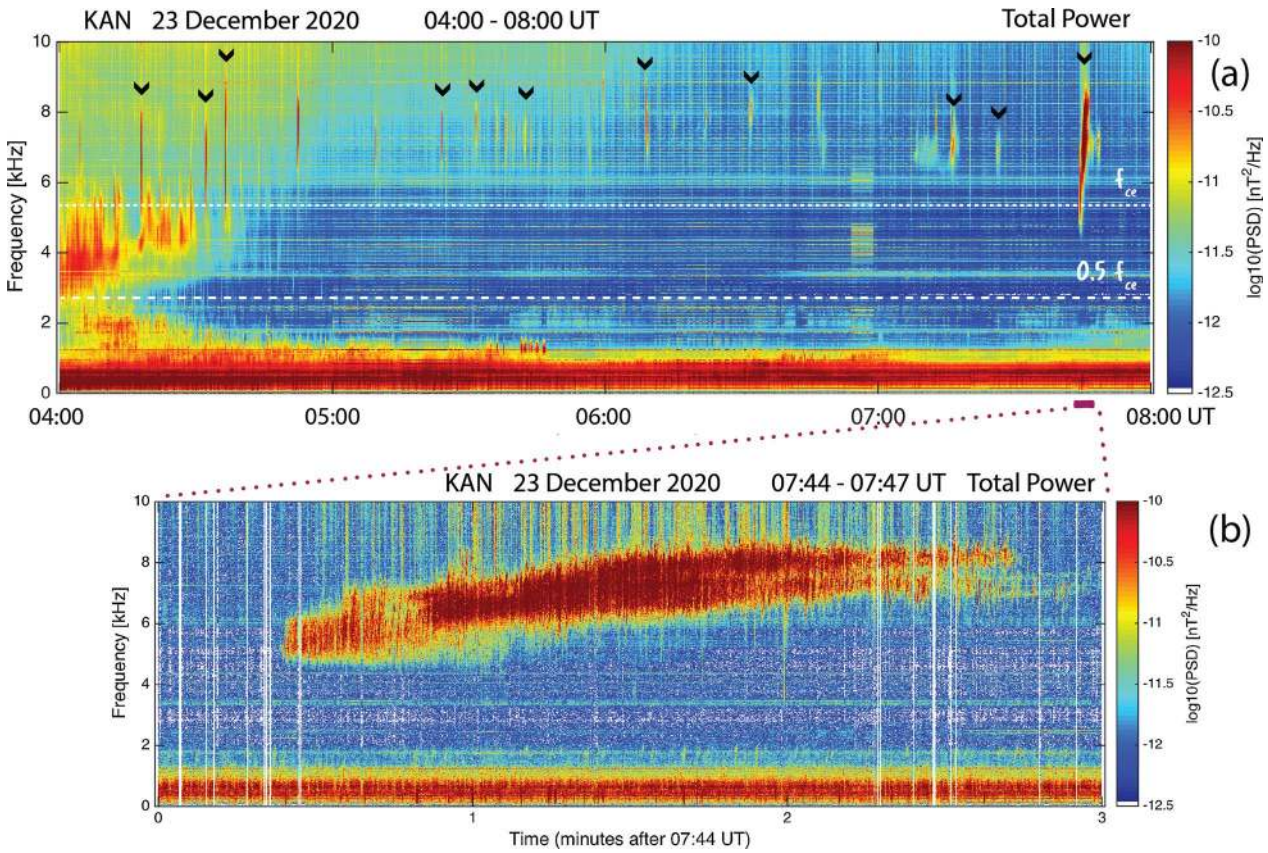

Fig. 4 Long lasting 'wands' VLF bursty-patches at KAN. Power spectrum density at KAN on 23 December 2020 from 04:00 to 08:00 UT (05:30–09:30 MLT) and from 07:44 to 07:47 UT, between 0 and 10 kHz. Dashed and dotted horizontal white lines show, respectively, the local equatorial 0.5 f_{ce} and f_{ce} for the L-shell of KAN. Through this panel we see multiple frequency-elongated VLF bursty-patches mostly for 6 < f < 8 kHz. As examples, some of these 'wands' are indicated with black angle arrows to make them more noticeable to the reader

emissions, it could partially explain the periodicity that is sometimes observed with these particular VLF bursty-patches.

Previous studies on long lasting QP emissions have found that the source region for QP emissions can be rather large and extend over several MLT (e.g., Martinez-Calderon et al. 2020; Němec et al. 2016; Titova et al. 2015). However, in these cases, the QP emissions not only show similar characteristics, but also changing characteristics with similar tendency, for example an increase or decrease in frequency or periodicity. For the 'wands' show here, those characteristics do not seem to apply. While they do remain at similar frequency bands, there does not seem to be any clear pattern in their shape or periodicity. Intermittent electron injections from the tail for several hours could maintain the instability responsible for the wave generation of these 'wands' and could explain the changes of intensity between bursts.

VLF bursty-patches with rising tones

Figure 5a shows the power spectrum density detected at KAN on 13 February 2021 from 05:00 to 09:00 UT (06:30–10:30 MLT) and for frequencies between 0 and 10 kHz. We note the presence of usual VLF hiss and chorus emissions below or centered on 0.5 f_{ce} for the entire time frame shown here. We focus on several VLF bursty-patches observed from ~ 05:40 to 08:00 UT above f_{ce}, mostly between 6 and 8.5 kHz. The first three bursts are indicated by black angle arrows. The first two bursts are centered at around 7 kHz lasting less than 10 min, while the third burst corresponds to a group of three separate rising tones at lower frequencies, just below the f_{ce} line at ~ 06:10 UT. We also observe a hiss-like burst starting at ~ 06:30 UT centered at ~ 7 kHz and showing multiple discrete rising tones. The variations in frequency of the envelope of this VLF bursty-patch is indicated by the black shaped arrow. We note these rising tones more easily at f ~ 8 kHz in the large burst just before 07:00 UT.

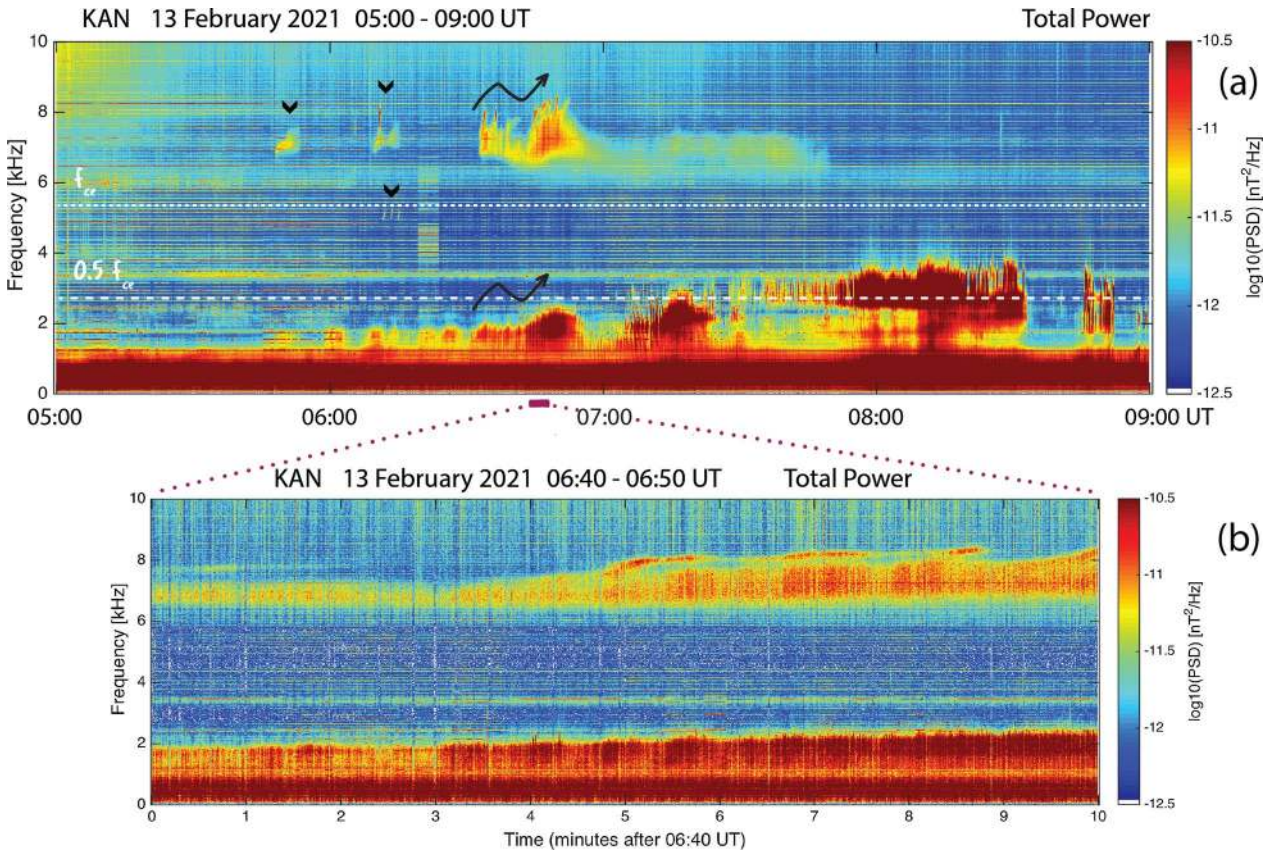

Fig. 5 Rising tone VLF bursty-patches at KAN. Power spectrum density at KAN on 13 February 2021 from **a** 05:00 to 09:00 UT (06:30–11:30 MLT) and from **b** 06:40 to 06:50 UT, between 0 and 10 kHz. Dashed and dotted horizontal white lines show, respectively, the local equatorial 0.5 f_{ce} and f_{ce} for the L-shell of KAN. Several VLF bursty-patches (black angle arrows and black shaped arrows) are observed above f_{ce}, particularly between 05:40 and 08:00 UT from 6 to 8.5 kHz. This event shows multiple hiss-like bursts with clear discrete rising tones

To see this more clearly, Fig. 5b shows us a 10-min time frame between 06:40 and 06:50 UT. In this close-up we note the unstructured hiss-like emission centered around 7 kHz with at least 3–4 discrete rising tones on top of the emission.

The group of VLF bursty-patches starting at ~ 05:40 UT and centered on 7 kHz, show some similarities with the chorus emissions observed at the same timings but below the 0.5 f_{ce} line. We note that the first two VLF bursty-patches starting at 05:40 and 06:15 UT seem to have the similar shapes to chorus bursts starting at the same times between 1 and 2 kHz. The largest VLF bursty-patch starting at 06:30 UT centered at f ~ 7 kHz and the corresponding chorus emissions below 2.5 kHz also appear to have similar envelope shape following the same frequency variations. This can be seen more clearly by comparing the two black shaped arrows indicating the evolution of the frequency envelope for the two emissions.

Unlike previous cases shown in this section, here we see elements that could suggest emissions observed below and above f_{ce} are at least, temporarily linked. If the VLF bursty-patches and the lower frequency chorus are related, it could point to a radially extended source region generating emissions with similar features propagating from lower and higher L-shells to KAN. If the emissions observed at higher frequencies correspond to harmonics of the chorus below 2.5 kHz, then we would expect the emissions to be observed at a maximum frequency of 7.5 kHz possibly corresponding to the third harmonic. This is clearly not the case here as the VLF bursty-patches with rising tones peak at much higher frequencies close to 8.3 kHz.

Quasi-periodic VLF bursty-patches

Figure 6 shows the power spectrum density observed at KAN on 20 January 2021 at two different time intervals: (a) 09:00–13:00 UT (10:30–14:40 MLT) and (b) 10:35–10:45 UT (11:35–11:45 MLT). Figure 6a shows the presence of multiple vertical lines between approximately 4 and 8 kHz. These lines seem to start around 09:30 UT

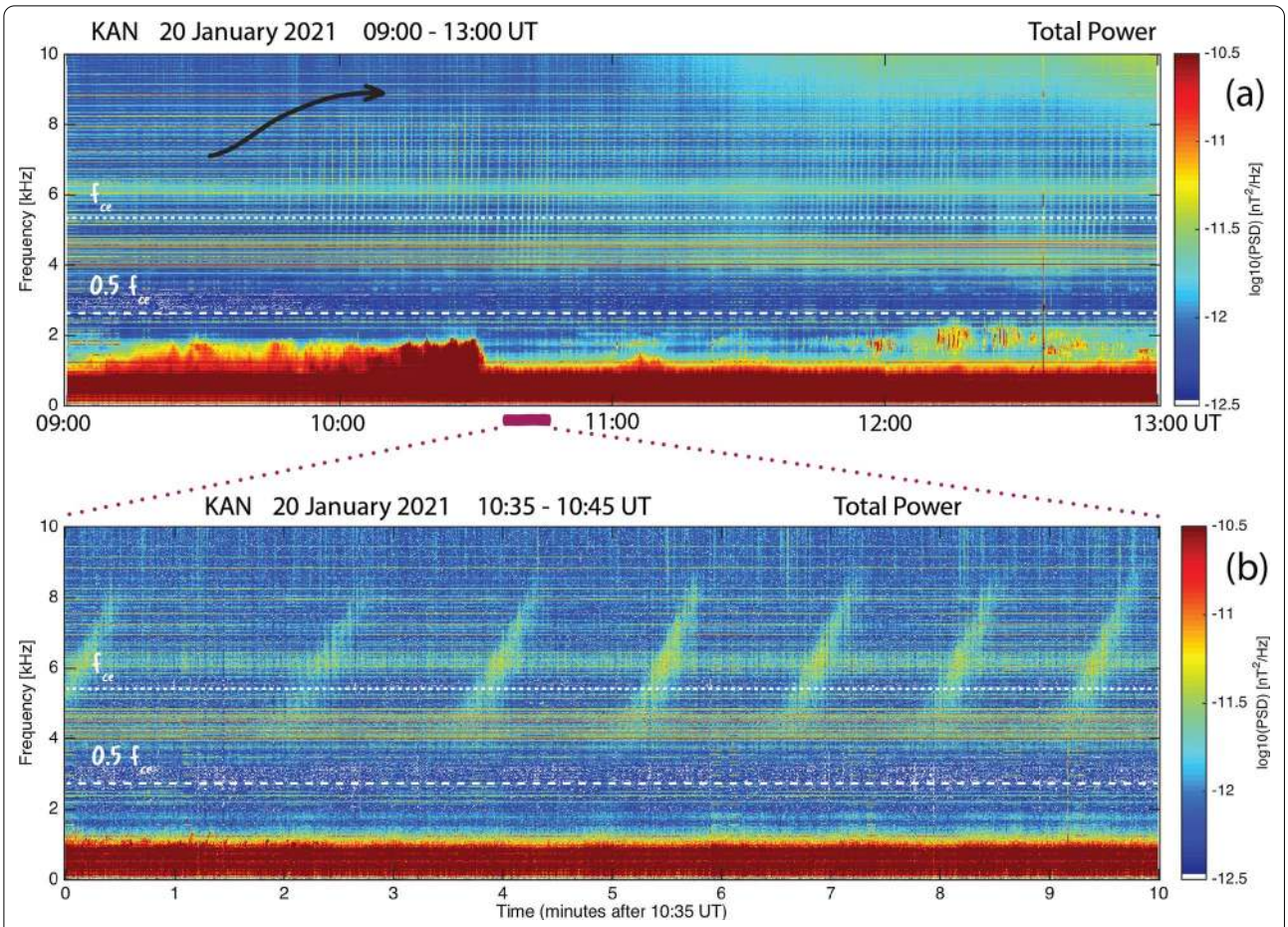

Fig. 6 Quasi-periodic VLF bursty-patches observed at KAN. Power spectrum density at KAN on 20 January 2021 from **a** 09:00 to 13:00 UT (10:30–14:30 MLT) and from **b** 10:35 to 10:45 UT, between 0 and 10 kHz. Dashed and dotted horizontal white lines show, respectively, the local equatorial 0.5 f_{ce} and f_{ce} for the L-shell of KAN. Long lasting quasi-periodic VLF bursty-patches are observed from ~ 09:30 UT between 4 and 9 kHz. In panel **a** they appear as vertical lines with a periodicity of a few minutes. A black shaped arrow is used to indicate the start and evolution of the emission envelope as a function of frequency. Panel **b** shows selected 10 min of the same emission at the timings indicated by the magenta line in panel (**a**). On panel **b** quasi-periodic features are clearly visible showing a periodicity of 1–2 min

centered on 6 kHz, just above the f_{ce} dotted line, and then extend in frequency with time. To make this clearer to the reader the approximate start of the event and the frequency evolution are indicated by a black shaped arrow in Fig. 6a. If we look closely, these vertical lines seem to have a periodicity of a few minutes and last until the end of the figure (~ 3.5 h).

Using Fig. 6b to observe this event more closely, we can clearly see that this VLF bursty patch emission shows the same spectral features as a 'usual' quasi-periodic emission with a period of 1 to 2 min. We also note that the emission is centered just above the f_{ce} line at ~ 6 kHz. This could correspond to a QP emission propagating from a source located at lower L-shells than KAN and lasting for several hours. As discussed at the end of the "'Wand' VLF bursty-patches" section, QP emissions have shown to be long-lasting and have large source regions. These type of VLF bursty-patch emissions are not uncommon at KAN, with QP emissions being frequently observed below f_{ce}.

When considering quasi-periodic VLF bursty-patches we have observed two types of cases. The first kind is where the emissions are clearly above the 0.5 f_{ce} or f_{ce} at KAN during the entire observation, and their elements seems relatively stable in frequency, as shown in Fig. 6. The other type is when we see QP elements at lower frequencies, usually around 0.5 f_{ce} that steadily start encompassing higher and higher frequencies ranges with time. In these cases, the QP elements can cover a range up to 10 or 12 kHz in a similar way as the bursts shown in Fig. 1. The large frequency ranges involved in the latter case, as well as those of the 'wands' in Sect. 4.3, suggest specific wave propagation features (fanning of the ray path, e.g., Martinez-Calderon et al. 2021) or unusual

source characteristics (possible radial expansion of the source) which need to be analyzed further.

S-shaped VLF bursty-patches

Figure 7 shows the power dynamic spectrum observed on 03 February 2021 at KAN for frequencies between 0 and 13 kHz at two different time frames: (a) 09:00 and 13:00 UT (10:30–14:30 MLT) and (b) 11:00–11:02 UT. This period is highly active as evidenced by the multiple VLF emissions observed during this time frame in Fig. 7a. White lines at frequencies above 12 kHz are due to strong Russian transmitters whose signal has been removed by the sferics filter. Figure 7a shows a period with very intense hiss emissions with bursts and chorus-like features at frequencies below 3 kHz ($< 0.5\, f_{ce}$). We also note multiple VLF bursts mixed with chorus emissions for $0.5\, f_{ce} < f < f_{ce}$. It appears that the bursts around 4 kHz have some correspondence with the chorus observed below $0.5\, f_{ce}$, we will, therefore, not consider these emissions as VLF bursty-patches ("Definition of VLF bursty-patches" section). There are also 2 groups of round VLF bursty-patches observed between 11:30 and 12:30 UT above 10 kHz, but since we already discussed these emissions in the "Rounded VLF bursty-patches" section we will not address them here. For this example, we will focus on 4 groups of S-shaped VLF bursty-patches observed at frequencies higher than 8 kHz and indicated by the black angle arrows in Fig. 7a. To get a better look at the bursts composing these groups, Fig. 7b shows a 2-min close up, where we can clearly see the S-shape of a single burst.

The first two groups are between $f = 8$ and 10 kHz and are observed between 09:15 and 10:00 UT. They appear to be made of 2–5 S-shaped bursts separated by intervals of a few minutes and have an increase of their top frequency with time. The second group seems to show a more hiss-like nature which could be due to smearing by the sferics filter or the time resolution of the figure, but the distinct bursts are still visible. The two other groups are observed from 10:30 to 11:20 UT between 9 and 13 kHz. In the latter groups, the bursts not only are more intense but also each element has a larger frequency range (1 to 2 kHz from lowest to highest frequency point). In the cases shown here, the number of S-shaped bursts is below 5. We noted that the number of S-shaped bursts in these type of VLF bursty-patches is commonly between 4 and 5. The mechanism behind this number

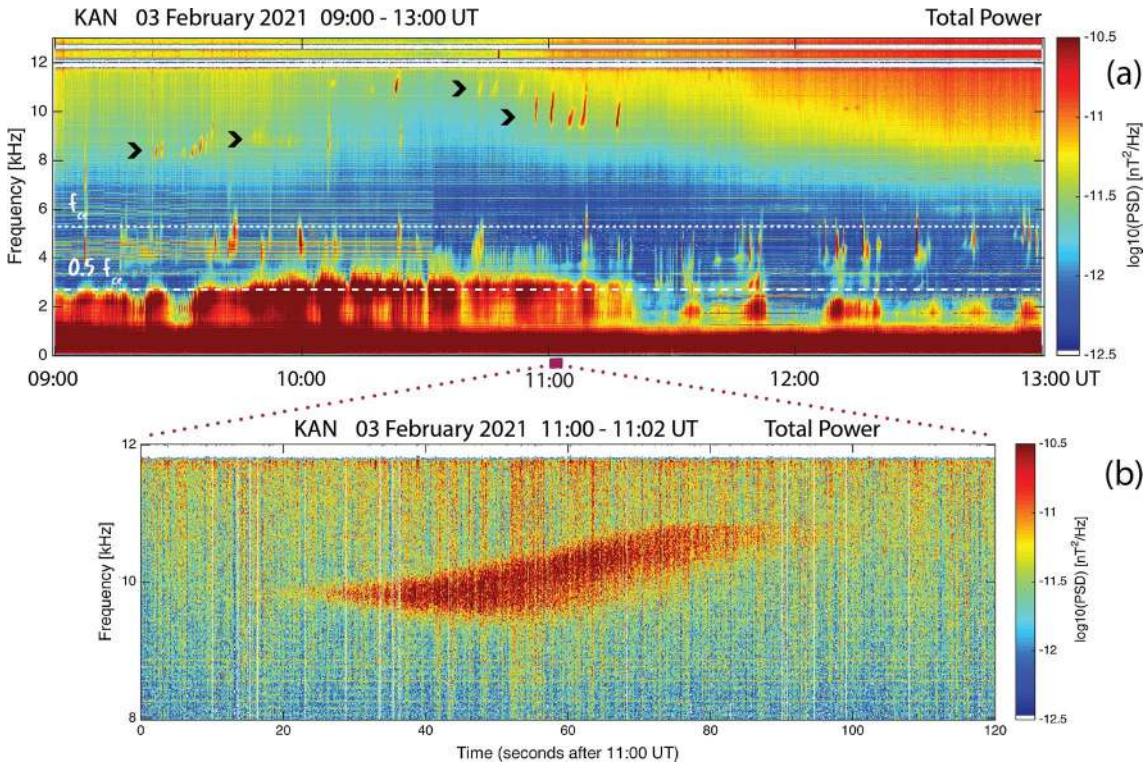

Fig. 7 S-shaped VLF bursty-patches observed at KAN. Power spectrum density at KAN on 03 February 2021 from 09:00 to 13:00 UT (10:30–14:30 MLT) between 0 and 13 kHz. Dashed and dotted horizontal white lines show, respectively, the local equatorial 0.5 f_{ce} and f_{ce} for the L-shell of KAN. S-shaped quasi-periodic VLF bursty-patches are observed in multiple groups above 8 kHz from ~ 09:15 UT to 11:20 UT. Each group is indicated by magenta arrows for easier identification. These emissions are characterized by smaller periodic groups of several S-shaped bursts

remains unknown, as is the process behind the changes in frequency between the first and last two groups.

'Bird' VLF bursty-patches

Figure 8 shows the power spectrum density observed at KAN for 19 January 2021 between (a) 09:00–13:00 UT (10:30–14:30 MLT) and (b) 12:00–12:10 UT, between 0 and 12 kHz. In this figure, we observe multiple hiss bands. The first and most intense band is below 1 kHz, with two additional weaker ones between 3–5 kHz and 5–7 kHz. The hiss band at higher frequencies is considered a VLF bursty-patch but we won't discuss it here, as we would like to focus on the events at higher frequencies. Indeed, in the approximately first and last hour of Fig. 8 we see two groups of 'Bird' VLF bursty-patches, mostly detected between 8 and 10 kHz. The approximate timings of observations of these events are indicated by magenta lines at the top of the spectrum. These emissions are characterized by multiple bursts that have spectral features resembling the shape of a cartoon bird seen from the side (e.g., Manninen et al. 2017, 2021). Indeed, with a little bit of imagination the VLF bursty-patches from 09:30 to 10:30 UT could even be seen as a peacock. However, as shown in Fig. 8b, in the time frame of several minutes, this shape is smeared out to resemble more of an elongated letter 'S'.

'Bird' VLF bursty-patches are usually seen in groups or at least 2 burst in less than 1 h. When observed in groups, they have a tendency to increase in frequency with time, but this is not a general rule. Within a group, their periodicity tends to remain fairly similar, suggesting the mechanisms behind their periodicity might be similar to those of more usual QP emissions.

Summary and conclusions

Using a sferics filter developed by SGO, we have been able to easily observe VLF waves propagating at frequencies higher than the local equatorial 0.5 f_{ce} at the L-shell

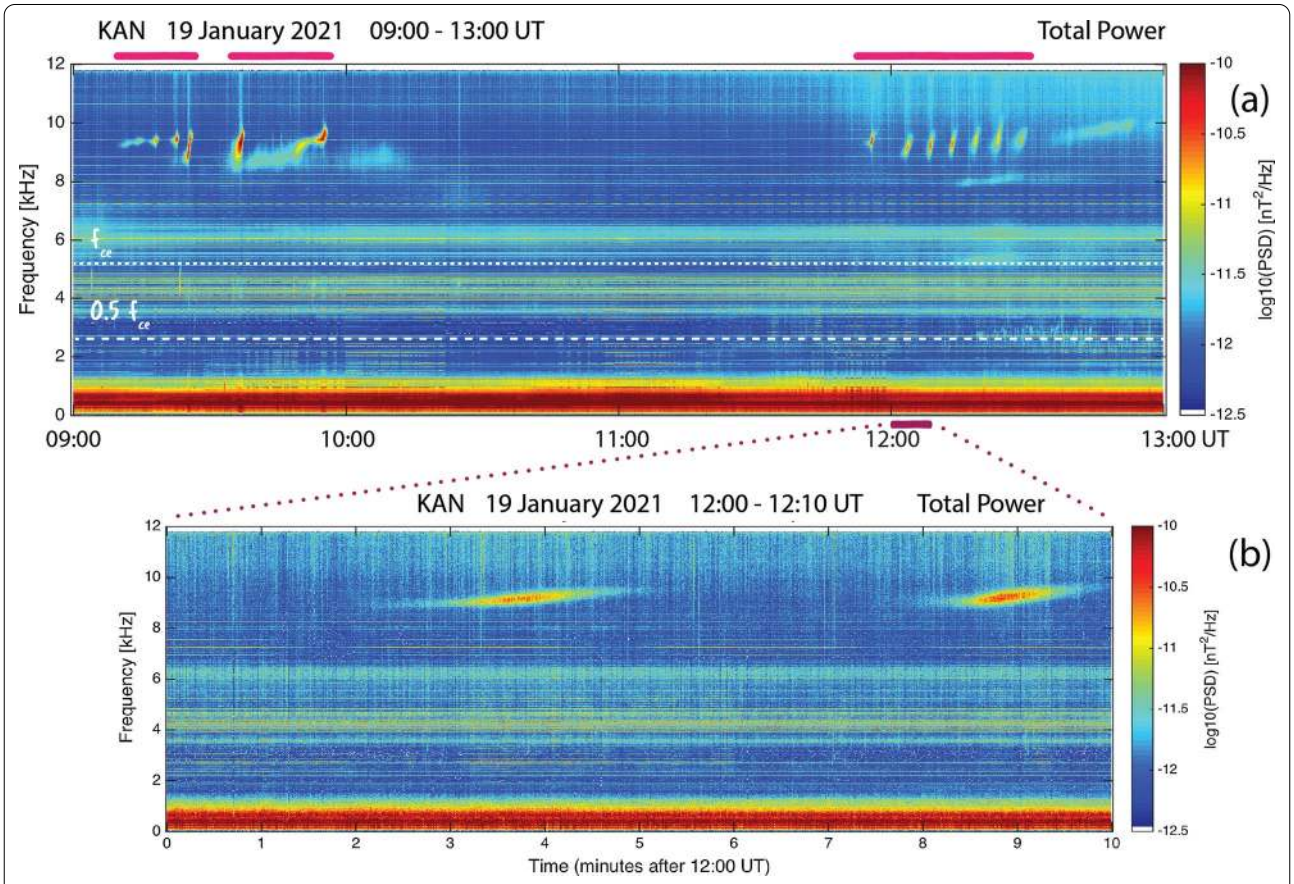

Fig. 8 'Bird'VLF bursty-patches observed at KAN. Power spectrum density at KAN on 19 January 2021 from **a** 09:00 to 13:00 UT (10:30–14:30 MLT) and from **b** 12:00 and 12:10 UT, between 0 and 12 kHz. Dashed and dotted horizontal white lines show, respectively, the local equatorial 0.5 f_{ce} and f_{ce} for the L-shell of KAN. 'Bird'VLF bursty-patches are observed in two distinct occasions from 09:05 to 10:15 UT between ~ 8.5 and 10 kHz and from 11:45 to 12:30 UT between ~ 9 and 10 kHz. These events show several bursts that have a distinctive cartoon bird shape. We also note some hiss-like VLF bursty-patches observed either between bursts or at the end of the events

of the ground station of KAN. Whistler-mode waves that reach the ground are thought to mostly propagate field aligned, ducted by the waveguide and, therefore, are limited to frequencies below the local $0.5\,f_{ce}$. Hence, for VLF bursty-patches to reach KAN they should have propagated unducted from lower L-shells, most likely fanning outwards from a source located at $L < 5.5$ (e.g., Martinez-Calderon et al. 2021). Another option would be for some kind of lateral propagation within the ionosphere before reaching an exit point close to KAN.

In this manuscript we finally unify the name of these emissions and settle it as VLF bursty-patches, with an established definition. We also present their most recent occurrence rates (2016–2021), and illustrate the different types of VLF bursty-patches that have been observed since 2019–2021. We also show how their characteristics change in time depending on their spectral features.

While these types of emissions have been reported before (Shiokawa et al. 2014; Manninen et al. 2016, 2021), we are still unaware of many of their properties, mechanisms behind their spectral features, and in particular their specific mode of propagation. We hope this manuscript will serve as the foundation for further studies on these type of waves.

Abbreviations

KAN: Kannuslehto ground-station (VLF receiver location); ELF: Extremely Low-Frequency emissions; VLF: Very-Low-Frequency emissions; QP: Quasi-periodic; SGO: Sodankylä Geophysical Observatory, University of Oulu; ATH: Athabasca ground-station (VLF receiver location); MLAT: Magnetic latitude; L: L-shell; kHz: Kilohertz; f: Frequency; f_{ce}: Local electron equatorial gyrofrequency; RREs: Recently revealed emissions; fT: Femto tesla (10^{-15} T); UT: Universal time (UT = MLT − 1.5 at KAN); MLT: Magnetic local time (MLT = UT + 1.5 at KAN.

Acknowledgements

All the VLF data from KAN is available as quick-plots at https://www.sgo.fi/pub_vlf/. Any additional data in other formats can be requested by contacting the PI of the instrument Jyrki Manninen. Claudia Martinez-Calderon would like to acknowledge Natalia Kleimenova for her previous work on VLF bursty-patches and her useful comments during the presentation of these results before the preparation of this manuscript. The authors would like to thank the Arcl International Visiting Grants from the University of Oulu for their travel support to Finland to work with the data in-situ. We also would like to acknowledge the support from the PWING project from Nagoya University.

Authors' information

CMC is an associate professor at Nagoya University and has been working with VLF emissions since 2013. JKM is the vice director of SGO, University of Oulu and has been studying VLF waves since 1990. He is now the PI of wideband VLF observations in Finland. JTM is a graduate student in Physics at the University of Oulu and has trained for two summers at SGO working with VLF data. TT has designed and built the receiver used at KAN and the filters for the analysis programs of KAN data.

Authors' contributions

CMC wrote the manuscript, visually inspected the data at KAN, and selected cases to present in this study. As PI of the instrument at KAN, JKM also made case selections and closely advised on the discussion and outline of this manuscript. JTM visually inspected the data for the 2019–2021 campaigns and compiled event lists. TT wrote the code allowing for the recording, plotting and data analysis of VLF emissions at KAN. TT is also responsible for the technique and code implemented in the sferics filter at KAN. All authors read and approved the final manuscript.

Funding

The instrumentation and data analysis are entirely funded by the Sodankylä Geophysical Observatory and the University of Oulu. CMC benefited from an Arcl International Visiting Grants from the University of Oulu that funded travel to Finland to work with the data in-situ. CMC research and analysis is funded by Nagoya University and the PWING project (JSPS 16H06286).

Availability of data and materials

Power spectrum density of VLF data for KAN is available at https://www.sgo.fi/pub_vlf/. Any additional data in other formats can be requested by contacting the PI of the instrument Jyrki Manninen.

Declarations

Ethics approval and consent to participate

Not applicable

Consent for publication

Not applicable

Competing interests

The authors declare that they have no competing interests.

Author details

[1]Institute for Space-Earth Environmental Research, Nagoya, Japan. [2]Sodankylä Geophysical Observatory, Sodankylä, Finland.

Received: 1 June 2021 Accepted: 7 September 2021
Published online: 19 October 2021

References

Barr R, Jones DL, Rodger C (2000) ELF and VLF radio waves. J Atmos Solar Terr Phys 62(17):1689–1718. https://doi.org/10.1016/S1364-6826(00)00121-8

Carpenter DL (1968) Ducted whistler-mode propagation in the magnetosphere; a half-gyrofrequency upper intensity cut-off and some associated wave growth phenomena. J Geophys Res Space Physics 73:2919–2928. https://doi.org/10.1029/JA073i009p02919

Gurnett DA, Bhattacharjee A (2017) Introduction to plasma physics: With space, laboratory and astrophysical applications. Cambridge University Press, Cambridge

Hayakawa M, Sazhin SS (1992) Mid-latitude and plasmaspheric hiss: a review. Planet Space Sci. https://doi.org/10.1016/0032-0633(92)90089-7

Helliwell RA (1965) Whistlers and related ionospheric phenomena. Stanford University Press, Stanford, Calif.

Inan US, Bell TF (1977) The plasmapause as a VLF wave guide. J Geophys Res Space Physics 82:2819–2827. https://doi.org/10.1029/JA082i019p02819

Kennel CF, Petschek H (1966) Limit on stably trapped particle fluxes. J Geophys Res Space Physics 71(1):1–28. https://doi.org/10.1029/JZ071i001p00001

Lichtenberger J, Ferencz C, Bodnar L, Hamar D, Steinbach P (2008) Automatic Whistler Detector and Analyzer system: Automatic Whistler Detector. J Geophys Res 113:A12201. https://doi.org/10.1029/2008JA013467

Lichtenberger J, Ferencz C, Hamar D, Steinbach P, Rodger CJ, Clilverd MA, Collier AB (2010) Automatic Whistler Detector and Analyzer system: implementation of the analyzer algorithm. J Geophys Res 115:A12214. https://doi.org/10.1029/2010JA015931

Manninen J, Turunen T, Kleimenova N, Rycroft M, Gromova L, Sirviö I (2016) Unusually high frequency natural VLF radio emissions observed during daytime in Northern Finland. Environ Res Lett 11(12):124006. https://doi.org/10.1088/1748-9326/11/12/124006

Manninen J, Turunen T, Kleimenova NG, Gromova LI, Kozlovskii AE (2017) A new type of daytime high-frequency VLF emissions at auroral latitudes ("bird emissions"). Geomag Aeron 57(1):32–39. https://doi.org/10.1134/S0016793217010091

Manninen J, Kleimenova N, Turunen T, Nikitenko A, Gromova L, Fedorenko Y (2021) New type of short high-frequency VLF patches ("VLF birds") above

4–5 kHz. J Geophys Res Space Physics. https://doi.org/10.1029/2020JA028601
Manninen J. (2005) Some aspects of ELF-VLF emissions in geophysical research. Ph.D Thesis, Oulu University. https://www.sgo.fi/Publications/SGO/thesis/ManninenJyrki.pdf
Martinez-Calderon C, Shiokawa K, Miyoshi Y, Ozaki M, Schofield I, Connors M (2015) Polarization analysis of VLF/ELF waves observed at subauroral latitudes during the VLF-chain campaign. Earth Planets Space 67(1):1–13. https://doi.org/10.1186/s40623-014-0178-7
Martinez-Calderon C, Shiokawa K, Miyoshi Y, Keika K, Ozaki M, Schofield I, Kurth WS (2016) ELF/VLF wave propagation at subauroral latitudes: conjugate observation between the ground and Van Allen Probes A.581. J Geophys Res Space Physics 121(A6):5384–5395. https://doi.org/10.1002/2015JA022264
Martinez-Calderon C, Katoh Y, Manninen J, Kasahara Y, Matsuda S, Kumamoto A et al (2020) Conjugate observations of dayside and nightside VLF chorus and QP emissions between Arase (ERG) and Kannuslehto, Finland. J Geophys Res Space Physics. https://doi.org/10.1029/2019JA026663
Martinez-Calderon C, Katoh Y, Manninen J, Santolik O, Kasahara Y, Matsuda S et al (2021) Multievent study of characteristics and propagation of naturally occurring ELF/VLF waves using high-latitude ground observations and conjunctions with the Arase satellite. J Geophys Res Space Physics. https://doi.org/10.1029/2020JA028682
Němec F, Santolík O, Parrot M, Pickett J, Hayosh M, Cornilleau-Wehrlin N (2013) Conjugate observations of quasi-periodic emissions by Cluster and Demeter spacecraft. J Geophys Res Space Physics 118(1):198–208. https://doi.org/10.1029/2012JA018380
Němec F, Bezděková B, Manninen J, Parrot M, Santolik O, Hayosh M, Turunen T (2016) Conjugate observations of a remarkable quasiperiodic event by the low-altitude DEMETER spacecraft and ground-based instruments. J Geophys Res Space Physics 121:8790–8803. https://doi.org/10.1002/2016JA022968
Ozaki M, Yagitani S, Nagano I, Hata Y, Yamagishi H, Sato N, Kadokura A (2008) Localization of VLF ionospheric exit point by comparison of multipoint ground-based observation with full-wave analysis. Polar Sci 2(4):237–249. https://doi.org/10.1016/j.polar.2008.09.001
Santolík O (2008) New results of investigations of whistler-mode chorus emissions. Nonlin Processes Geophys 15:621–630. https://doi.org/10.5194/npg-15-621-2008
Sazhin SS, Hayakawa M (1992) Magnetospheric chorus emissions: a review. Planet Space Sci 40(5):681–697. https://doi.org/10.1016/0032-0633(92)90009-D
Sazhin S, Hayakawa M (1994) Periodic and quasiperiodic VLF emissions. J Atmos Terr Phys 56(6):735–753. https://doi.org/10.1016/0021-9169(94)90130-9
Sazhin SS, Bullough K, Hayakawa M (1993) Auroral hiss: a review. Planet Space Sci 41(2):153–166. https://doi.org/10.1016/0032-0633(93)90045-4
Shiokawa K, Yokoyama Y, Ieda A, Miyoshi Y, Nomura R, Lee S, Connors M (2014) Ground-based ELF/VLF chorus observations at subauroral latitudes VLF-chain campaign. J Geophys Res Space Physics 119:7363–7379. https://doi.org/10.1002/2014JA020161
Smith AJ, Engebretson MJ, Klatt EM, Inan US, Arnoldy RL, Fukunishi H (1998) Periodic and quasiperiodic ELF/VLF emissions observed by an array of Antarctic stations. J Geophys Res 103(A10):23611–23622. https://doi.org/10.1029/98JA01955
Titova E, Kozelov B, Demekhov A, Manninen J, Santolik O, Kletzing C, Reeves G (2015) Identification of the source of quasiperiodic VLF emissions using ground-based and Van Allen probes satellite observations. Geophys Res Lett 42:6137–6145. https://doi.org/10.1002/2015GL064911
Titova EE, Demekhov AG, Manninen J, Pasmanik DL, Larchenko AV (2017) Localization of the sources of narrow-band noise VLF emissions in the range 4–10 kHz from simultaneous ground-based and Van Allen Probes satellite observations. Geomag Aeron 57(6):706–718. https://doi.org/10.1134/S0016793217060135

Publisher's Note